

Heteroleptic Copper(I) Complexes Prepared from Phenanthroline and Bis-Phosphine Ligands

Adrien Kaeser,^{†,‡} Meera Mohankumar,[†] John Mohanraj,[§] Filippo Monti,[§] Michel Holler,[†] Juan-José Cid,[†] Omar Moudam,^{†,‡} Iwona Nierengarten,^{†,||} Lydia Karmazin-Brelot,^{||} Carine Duhayon,[‡] Béatrice Delavaux-Nicot,^{*,‡} Nicola Armaroli,^{*,§} and Jean-François Nierengarten^{*,†}

[†]Laboratoire de Chimie des Matériaux Moléculaires, Université de Strasbourg et CNRS (UMR 7509), 25 rue Becquerel, 67087 Strasbourg Cedex 2, France

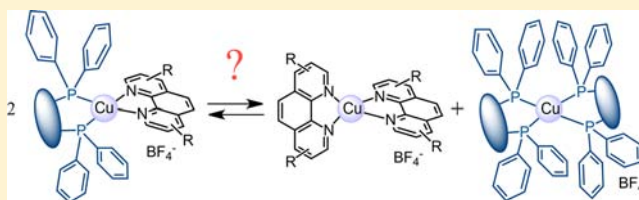
[§]Istituto per la Sintesi Organica e la Fotoreattività, Consiglio Nazionale delle Ricerche, Via Gobetti 101, 40129 Bologna, Italy

^{||}Service de Radiocristallographie, Institut de Chimie, Université de Strasbourg, 1 rue Blaise Pascal, B.P. 296/R8, 67008 Strasbourg Cedex, France

[‡]Laboratoire de Chimie de Coordination du CNRS (UPR 8241), Université de Toulouse (UPS, INPT), 205 Route de Narbonne, 31077 Toulouse Cedex 4, France

S Supporting Information

ABSTRACT: Preparation of $[\text{Cu}(\text{NN})(\text{PP})]^+$ derivatives has been systematically investigated starting from two libraries of phenanthroline (NN) derivatives and bis-phosphine (PP) ligands, namely, (A) 1,10-phenanthroline (phen), neocuproine (2,9-dimethyl-1,10-phenanthroline, dmp), bathophenanthroline (4,7-diphenyl-1,10-phenanthroline, Bphen), 2,9-diphenethyl-1,10-phenanthroline (dpep), and 2,9-diphenyl-1,10-phenanthroline (dpp); (B) bis(diphenylphosphino)methane (dppm), 1,2-bis(diphenylphosphino)ethane (dppe), 1,3-bis(diphenylphosphino)propane (dppp), 1,2-bis(diphenylphosphino)benzene (dppb), 1,1'-bis(diphenylphosphino)ferrocene (dppFc), and bis[(2-diphenylphosphino)phenyl] ether (POP). Whatever the bis-phosphine ligand, stable heteroleptic $[\text{Cu}(\text{NN})(\text{PP})]^+$ complexes are obtained from the 2,9-unsubstituted-1,10-phenanthroline ligands (phen and Bphen). By contrast, heteroleptic complexes obtained from dmp and dpep are stable in the solid state, but a dynamic ligand exchange reaction is systematically observed in solution, and the homoleptic/heteroleptic ratio is highly dependent on the bis-phosphine ligand. Detailed analysis revealed that the dynamic equilibrium resulting from ligand exchange reactions is mainly influenced by the relative thermodynamic stability of the different possible complexes. Finally, in the case of dpp, only homoleptic complexes were obtained whatever the bis-phosphine ligand. Obviously, steric effects resulting from the presence of the bulky phenyl rings on the dpp ligand destabilize the heteroleptic $[\text{Cu}(\text{NN})(\text{PP})]^+$ complexes. In addition to the remarkable thermodynamic stability of $[\text{Cu}(\text{dpp})_2]\text{BF}_4$, this negative steric effect drives the dynamic complexation scenario toward almost exclusive formation of homoleptic $[\text{Cu}(\text{NN})_2]^+$ and $[\text{Cu}(\text{PP})_2]^+$ complexes. This work provides the definitive rationalization of the stability of $[\text{Cu}(\text{NN})(\text{PP})]^+$ complexes, marking the way for future developments in this field.



INTRODUCTION

Cu(I) complexes prepared from phosphines and ligands such as 2,2'-bipyridine (bipy) or 1,10-phenanthroline (phen) were first investigated in detail more than 30 years ago.^{1,2} Initially, such systems generally prepared with PPh_3 as the P ligands looked promising because they exhibit long excited state lifetimes upon light excitation both in the solid state and in frozen solution.¹ They also display interesting photochemical properties in relation to bimolecular photoinduced electron transfer.² However, detailed studies have shown that exciplex quenching is important even for compounds incorporating bulky phosphines such as PPh_3 .¹ Moreover, the speciation of these compounds was hard to control even in noncoordinating solvents such as CH_2Cl_2 .¹ Subsequently, McMillin and co-workers reported mixed-ligand Cu(I) complexes prepared from

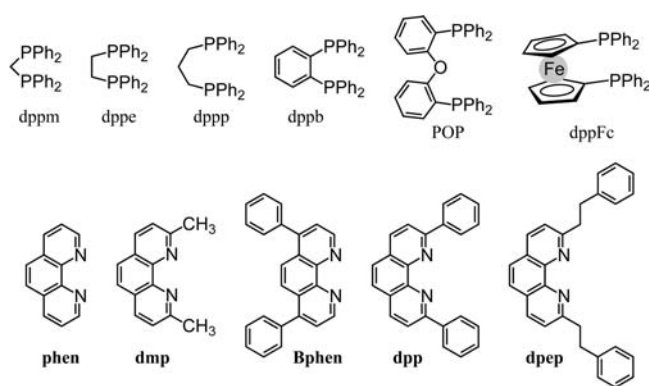
1,10-phenanthroline derivatives and bis[2-(diphenylphosphino)phenyl]ether (POP).^{3,4} Not only is ligand dissociation essentially suppressed for complexes prepared from this particular chelating bis-phosphine ligand⁴ but also these compounds are characterized by remarkably high emission quantum yields from their long-lived metal-to-ligand charge transfer (MLCT) excited state. Following this key finding, numerous examples of related heteroleptic Cu(I) complexes have been prepared from bis-phosphine and aromatic diimine ligands.^{6–9} Their outstanding emission properties have been exploited to produce efficient light-emitting devices, thus showing that inexpensive and earth-abundant Cu(I) is an

Received: August 2, 2013

Published: October 1, 2013

attractive alternative to noble metal ions for such applications.^{7,8} As part of this research, our groups investigated heteroleptic Cu(I) complexes combining various phenanthroline derivatives (NN) with different bis-phosphine ligands (PP).^{8,10–12} During the course of these studies, it was found that an equilibrium between the homoleptic and the heteroleptic complexes is sometimes observed in solution. This represents actually a major limitation for preparation of stable $[\text{Cu}(\text{NN})(\text{PP})]^+$ derivatives.¹³ We thus became interested in a deeper understanding of the structural parameters influencing the stability of these compounds and decided to systematically investigate their preparation starting from the libraries of phenanthroline derivatives and PP ligands depicted in Chart 1.

Chart 1. Libraries of NN Derivatives and PP Ligands Used for Preparation of Heteroleptic $[\text{Cu}(\text{NN})(\text{PP})]^+$ Derivatives

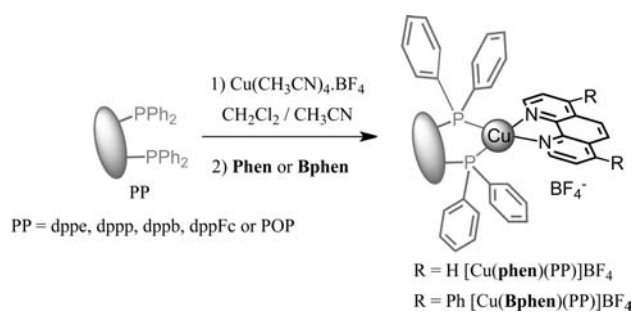


RESULTS AND DISCUSSION

The six selected bis-phosphine ligands (dppm, dppe, dppp, dppb, dppFc, and POP) are all commercially available as well as 1,10-phenanthroline (phen), neocuproine (2,9-dimethyl-1,10-phenanthroline, dmp), and bathophenanthroline (4,7-diphenyl-1,10-phenanthroline, Bphen). 2,9-Diphenylethyl-1,10-phenanthroline¹⁴ (dpep) and 2,9-diphenyl-1,10-phenanthroline^{8,15} (dpp) were prepared according to reported procedures.

2,9-Unsubstituted-1,10-phenanthroline Derivatives (phen and Bphen). Treatment of phen with an equimolar amount of the appropriate bis-phosphine ligand (dppe, dppp, dppb, POP, or dppFc) and $\text{Cu}(\text{CH}_3\text{CN})_4\text{BF}_4$ in $\text{CH}_2\text{Cl}_2/\text{CH}_3\text{CN}$ gave the corresponding $[\text{Cu}(\text{phen})(\text{PP})]\text{BF}_4$ derivatives (Scheme 1). ^1H NMR analysis of the crude mixtures thus obtained indicated formation of a single complex in all cases.

Scheme 1. Preparation of Heteroleptic $[\text{Cu}(\text{NN})(\text{PP})]^+$ Derivatives from phen and Bphen



The heteroleptic complexes were then isolated in a pure form by recrystallization in $\text{CH}_2\text{Cl}_2/\text{Et}_2\text{O}$. Similar results were obtained when Bphen was used as the NN ligand; the $[\text{Cu}(\text{Bphen})(\text{PP})]\text{BF}_4$ complexes were thus prepared in excellent isolated yields.

The $[\text{Cu}(\text{phen})(\text{PP})]\text{BF}_4$ and $[\text{Cu}(\text{Bphen})(\text{PP})]\text{BF}_4$ complexes were characterized by ^1H , ^{13}C , and ^{31}P NMR spectroscopies, mass spectrometry, and elemental analysis. Typical examples of ^1H and ^{31}P NMR spectra are shown in Figure 1. For all compounds the ^{31}P NMR spectrum recorded at room temperature revealed a single resonance for the two equivalent P atoms of the chelating PP ligand. Cooling the samples to -60°C did not give rise to significant changes, and no additional signals could be detected. ^1H NMR spectra were also consistent with the proposed structures. Analysis of the integration of the ^1H NMR spectra revealed that, in all cases, both PP and NN ligands are present in a 1:1 ratio. As shown in Figure 1, a slight line broadening is observed for the ^1H NMR resonance of the phenanthroline proton H(2) of all complexes; this effect is most likely due to the proximity of the quadrupolar $^{63/65}\text{Cu}$ nuclei.¹⁶ In contrast, all other signals in the ^1H NMR spectra of complexes $[\text{Cu}(\text{NN})(\text{PP})]\text{BF}_4$ (NN = phen or Bphen) are well resolved and show no signs of broadening.

It can also be noted that the signal of proton H(2) is shielded in $[\text{Cu}(\text{Bphen})(\text{PP})]\text{BF}_4$ when compared to the corresponding signal in Bphen as a result of the ring current effect of the phenyl groups of the PP ligand on this particular proton. Shielding ranges from 0.4 to 0.9 ppm, the most important one being observed with dppb. Actually, since the bite angles are different for each of the chelating PP ligands, the relative orientation of the phenyl groups is not the same in the various complexes; thus, the effect on the chemical shift of H(2) is specific for each PP ligand. Importantly, the NMR spectra indicate also that there is no significant ligand exchange in solution leading to formation of the corresponding homoleptic species. Finally, the structure of all complexes was confirmed by FAB mass spectrometry. For all compounds the mass spectrum displays a singly charged ion peak assigned to $[\text{Cu}(\text{NN})(\text{PP})]^+$. Other minor peaks corresponding to $[\text{Cu}(\text{NN})]^+$ and $[\text{Cu}(\text{PP})]^+$ are also systematically observed in the mass spectra.

X-ray-quality crystals of $[\text{Cu}(\text{phen})(\text{dppb})]\text{BF}_4$ were obtained by vapor diffusion of Et_2O into a CH_2Cl_2 solution of the complex. As shown in Figure 2, the copper atom is in a highly distorted tetrahedral environment in which both the phenanthroline and the dppb are chelating ligands. The distortion mainly arises from the restricted chelate bite angles of both ligands ($\text{P}(1)-\text{Cu}(1)-\text{P}(2)$ $88.11(3)^\circ$ and $\text{N}(1)-\text{Cu}(1)-\text{N}(2)$ $81.9(1)^\circ$). The angle between the planes $\text{P}(1)-\text{Cu}(1)-\text{P}(2)$ and $(\text{N}1)-\text{Cu}(1)-(\text{N}2)$ is $85.62(7)^\circ$, and the bridging phenyl ring of dppb is tilted by ca. 31.6° with respect to the $\text{P}(1)-\text{Cu}(1)-\text{P}(2)$ plane.

Inspection of the crystal packing reveals a dimeric arrangement of the $[\text{Cu}(\text{phen})(\text{dppb})]^+$ cations in which the phenanthroline ligands partially overlay one another; the average distance between the mean planes of the two phenanthroline ligands is ca. 3.5 \AA (Figure 2). A similar arrangement has been already reported for X-ray crystal structures of $[\text{Cu}(\text{phen})(\text{POP})]\text{BF}_4$ ³ and $[\text{Cu}(\text{phen})(\text{dppFc})]\text{BF}_4$.¹⁰ In all cases the components of the pair are related to one another through a center of inversion that is located between the planes of the phenanthroline rings. As shown in Figure 2, two notable $\text{C}-\text{H}/\pi$ intermolecular interactions are also observed between neighboring $[\text{Cu}(\text{phen})(\text{dppb})]^+$ cations.

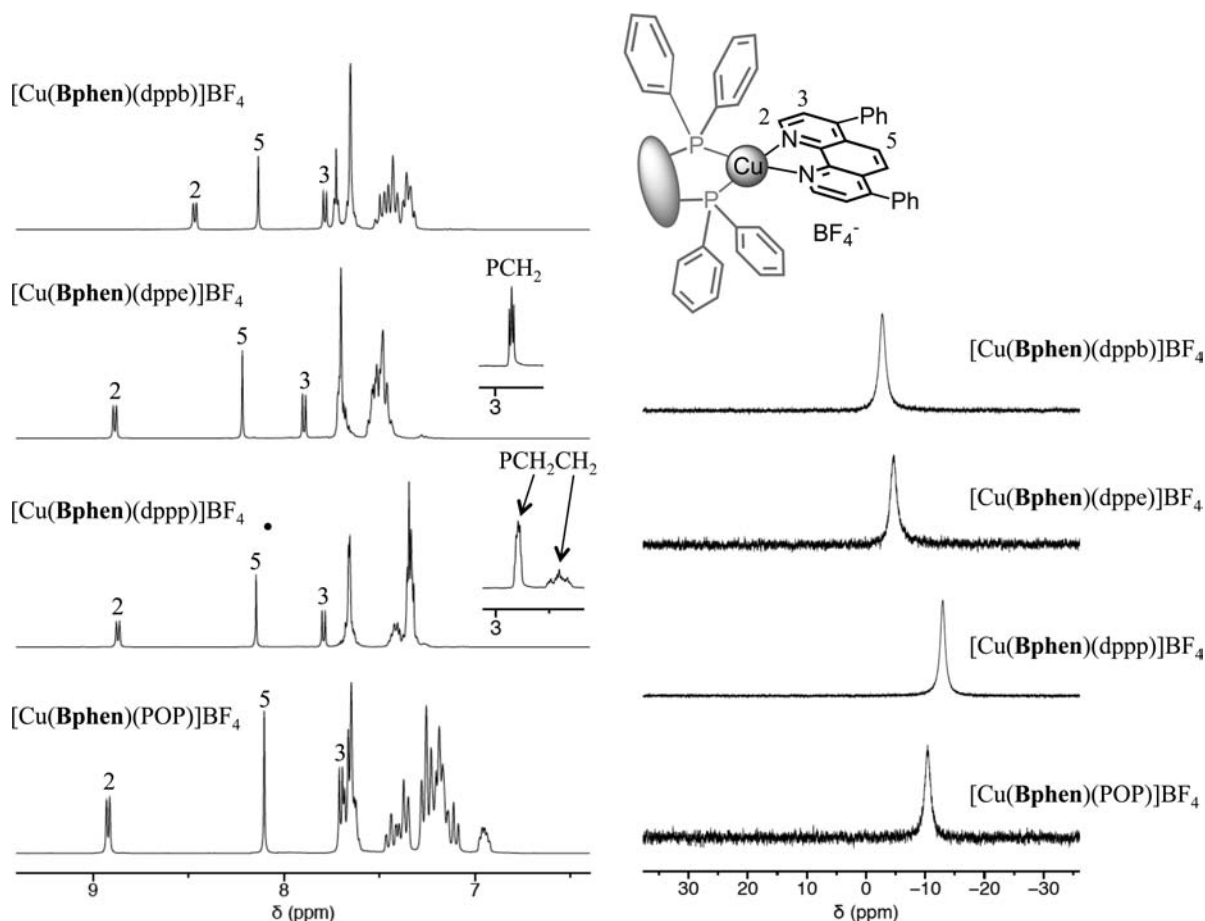


Figure 1. ^1H (left) and $^{31}\text{P}\{^1\text{H}\}$ (right) NMR spectra of $[\text{Cu}(\text{Bphen})(\text{PP})]^+\text{BF}_4^-$ (PP = dppb, dpe, dpp, and POP) recorded in CD_2Cl_2 at room temperature.

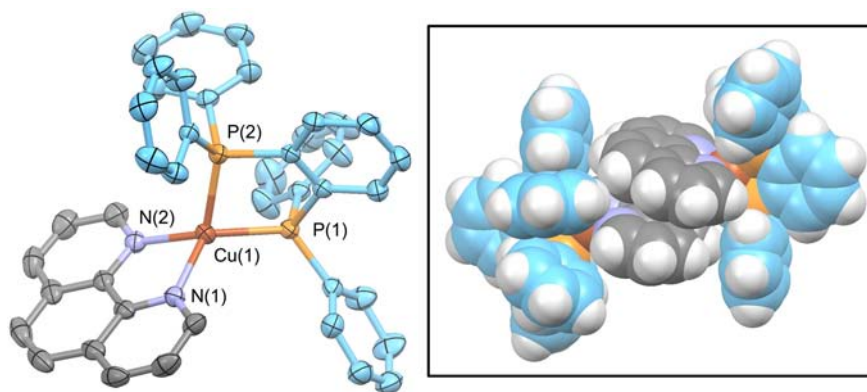


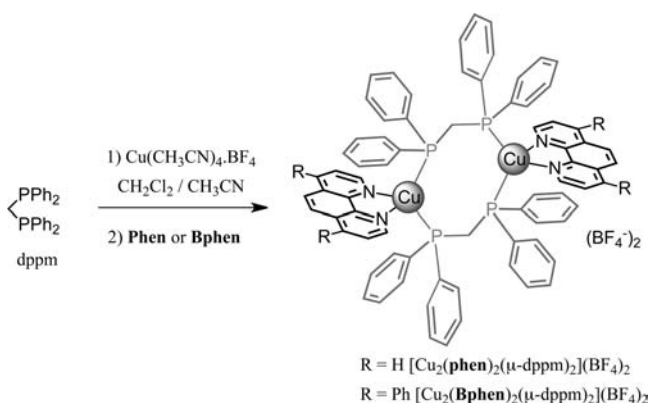
Figure 2. Structure of $[\text{Cu}(\text{phen})(\text{dppb})]^+\text{BF}_4^-$ (H atoms and counteranion are omitted for clarity; thermal ellipsoids are drawn at the 50% probability level). (Inset) Pairwise stacking of the phenanthroline ligands of neighboring $[\text{Cu}(\text{phen})(\text{dppb})]^+$ cations. Selected bond lengths (Angstroms): Cu(1)–P(1) 2.2381(9), Cu(1)–P(2) 2.2486(9), Cu(1)–N(1) 2.040(2), Cu(1)–N(2) 2.049(2). Selected bond angles (degrees): P(1)–Cu(1)–P(2) 88.11(3), P(1)–Cu(1)–N(1) 124.61(7), P(1)–Cu(1)–N(2) 129.37(7), P(2)–Cu(1)–N(1) 120.88(7), P(2)–Cu(1)–N(2) 116.11(8), N(1)–Cu(1)–N(2) 81.9(1).

These interactions involve one hydrogen atom of the phenanthroline unit and a phenyl group of the dppb ligand belonging to the neighboring cations. These phenanthroline hydrogen atoms are located at 2.8 Å from the center of their neighboring phenyl ring.

In the particular case of dppm, reaction with an equimolar amount of $\text{Cu}(\text{CH}_3\text{CN})_4\text{BF}_4$ and phen in $\text{CH}_2\text{Cl}_2/\text{CH}_3\text{CN}$ gave the dinuclear complex $[\text{Cu}_2(\text{phen})_2(\mu\text{-dppm})_2](\text{BF}_4)_2$

(Scheme 2). Similarly, $[\text{Cu}_2(\text{Bphen})_2(\mu\text{-dppm})_2](\text{BF}_4)_2$ was obtained when the reaction was performed with Bphen. Indeed, dppm can chelate metals, but the four-membered ring in such complexes is strained, and the ligand has a greater tendency to act either as a monodentate ligand or as a bridging bidentate ligand.¹⁷ Whereas a few examples of Cu(I) complexes in which dppm is a chelate ligand have been reported,¹¹ dinuclear Cu(I) complexes with two bridging dppm ligands are by far more

Scheme 2. Preparation of $[\text{Cu}_2(\text{phen})_2(\mu\text{-dppm})_2](\text{BF}_4)_2$ and $[\text{Cu}_2(\text{Bphen})_2(\mu\text{-dppm})_2](\text{BF}_4)_2$



common.^{18,19} It is also interesting to note that the chelating tendency of the $\text{Ph}_2\text{P}(\text{CH}_2)_n\text{PPh}_2$ ligands observed for $n = 2$ and 3 in the particular case of these Cu(I) complexes decreases when the chain length further increases. Effectively, dinuclear complexes have been reported for 1,4-bis(diphenylphosphino)butane ($n = 4$).⁵

Dinuclear complexes were characterized by NMR spectroscopy, mass spectrometry, and elemental analysis. ^1H and ^{31}P NMR spectra of $[\text{Cu}_2(\text{Bphen})_2(\mu\text{-dppm})_2](\text{BF}_4)_2$ recorded in CD_2Cl_2 at room temperature are depicted in Figure 3. In addition to the signals corresponding to phenyl groups of the dppm moieties, the ^1H NMR spectrum of $[\text{Cu}_2(\text{Bphen})_2(\mu\text{-dppm})_2](\text{BF}_4)_2$ is characterized by four sets of signals in a typical pattern for a 4,7-diphenyl-1,10-phenanthroline and a broad singlet at $\delta = 3.88$ ppm for the dppm ligands. ^{31}P NMR of this compound gave a broad singlet signal at room temperature ($\delta = -6.62$ ppm, $\Delta\nu_{1/2} = 216$ Hz). Cooling the sample to 200 K did not give rise to additional peaks, and no couplings were observed (e.g., $^2J_{\text{P-C-P}}$ or $^2J_{\text{P-Cu-P}}$) at all temperatures. This shows that the four P atoms are chemically and magnetically equivalent; thus, it can be deduced that the compound remains intact in solution.

For $[\text{Cu}_2(\text{Bphen})_2(\mu\text{-dppm})_2](\text{BF}_4)_2$, crystals suitable for X-ray crystal structure analysis were obtained by slow diffusion of

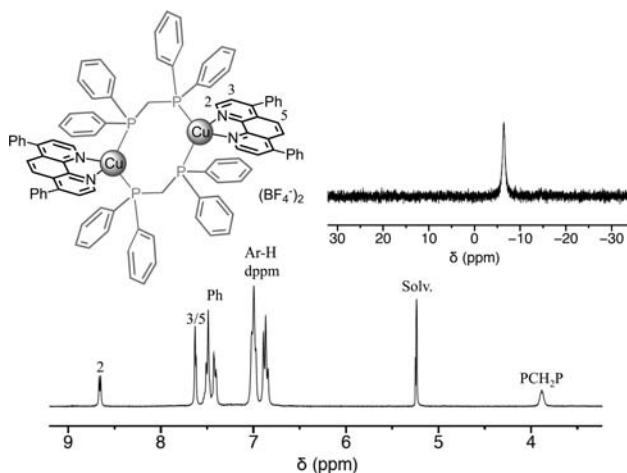


Figure 3. ^1H (bottom) and $^{31}\text{P}\{^1\text{H}\}$ (top right) NMR spectra of $[\text{Cu}_2(\text{Bphen})_2(\mu\text{-dppm})_2](\text{BF}_4)_2$ recorded in CD_2Cl_2 at room temperature.

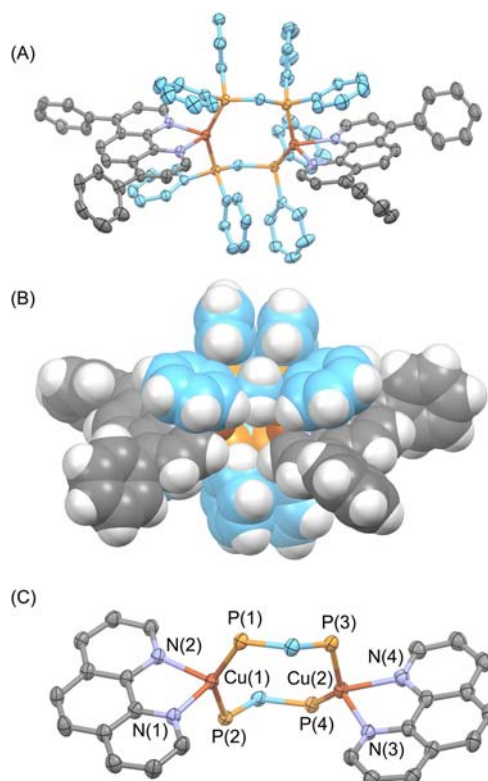


Figure 4. (A) Structure of $[\text{Cu}_2(\text{Bphen})_2(\mu\text{-dppm})_2](\text{BF}_4)_2 \cdot \text{CH}_2\text{Cl}_2$ (H atoms, counteranions, and CH_2Cl_2 molecule are omitted for clarity; thermal ellipsoids of the ORTEP plot are drawn at the 50% probability level). (B) CPK representation of the $[\text{Cu}_2(\text{Bphen})_2(\mu\text{-dppm})_2]$ dication highlighting the intramolecular $\pi\text{-}\pi$ interactions. (C) Details of the coordination sphere around the Cu(I) cations in the structure of $[\text{Cu}_2(\text{Bphen})_2(\mu\text{-dppm})_2](\text{BF}_4)_2 \cdot \text{CH}_2\text{Cl}_2$.

Et_2O into a CH_2Cl_2 solution of the complex. Two views of the $[\text{Cu}_2(\text{Bphen})_2(\mu\text{-dppm})_2]^{2+}$ dication are shown in Figure 4. Selected bond lengths and angles are summarized in Table 1. The two dppm moieties are bridging two $[\text{Cu}(\text{Bphen})]^+$ cations, thus forming an eight-membered $\text{Cu}_2\text{P}_4\text{C}_2$ metallacycle. With a $\text{Cu}(1)\text{-Cu}(2)$ distance of 4.4640(4) Å, there are no Cu–Cu interactions in $[\text{Cu}_2(\text{Bphen})_2(\mu\text{-dppm})_2]^{2+}$. Notable intramolecular $\pi\text{-}\pi$ interactions involve two phenyl rings

Table 1. Bond Distances (Angstroms) and Bond Angles (degrees) within the Coordination Sphere of $[\text{Cu}_2(\text{Bphen})_2(\mu\text{-dppm})_2](\text{BF}_4)_2 \cdot \text{CH}_2\text{Cl}_2$ (see Figure 4 for numbering)

selected bond lengths		selected bond angles	
Cu(1)–P(1)	2.2183(8)	P(1)–Cu(1)–P(2)	141.34(3)
Cu(1)–P(2)	2.2369(8)	P(1)–Cu(1)–N(1)	105.86(7)
Cu(1)–N(1)	2.091(2)	P(1)–Cu(1)–N(2)	108.25(7)
Cu(1)–N(2)	2.081(2)	P(2)–Cu(1)–N(1)	103.49(7)
Cu(2)–P(3)	2.2845(8)	P(2)–Cu(1)–N(2)	101.25(7)
Cu(2)–P(4)	2.2296(8)	N(1)–Cu(1)–N(2)	79.70(9)
Cu(2)–N(3)	2.081(2)	P(3)–Cu(2)–P(4)	134.83(3)
Cu(2)–N(4)	2.130(2)	P(3)–Cu(2)–N(3)	97.69(7)
		P(3)–Cu(2)–N(4)	98.25(7)
		P(4)–Cu(2)–N(3)	122.56(7)
		P(4)–Cu(2)–N(4)	108.04(7)
		N(3)–Cu(2)–N(4)	79.10(9)

within both of the dppm ligands. The average distance between the mean planes of the aromatic rings is ca. 3.6 Å in both cases. In addition, two intramolecular face-to-face π - π interactions are also observed between both phenanthroline ligands and a phenyl unit of one of their neighboring PPh₂ moieties. Establishment of these interactions is at the origin of the particularly large P-Cu-P angles. As a result, the metallacycle adopts a peculiar folded conformation and both phenanthrolines are no longer in a relative face-to-face orientation as typically observed in the X-ray crystal structures of related compounds.¹⁹

2,9-Disubstituted-1,10-phenanthroline Derivatives (dmp, dpep, and dpp). Reaction of dmp, dpep, and dpp with the PP ligands and Cu(CH₃CN)₄BF₄ was systematically investigated. A solution of the appropriate bis-phosphine ligand (1 equiv) and Cu(CH₃CN)₄BF₄ (1 equiv) in CH₂Cl₂/CH₃CN was stirred for 0.5 h; then dmp, dpep, or dpp (1 equiv) was added. After 1 h, solvents were evaporated. Products were analyzed as received by ¹H NMR. The relative proportion of the different possible complexes, i.e., [Cu(NN)(PP)]BF₄, [Cu(NN)₂]BF₄, and [Cu(PP)₂]BF₄, was deduced from comparison with the ¹H NMR spectrum of the corresponding [Cu(NN)₂]BF₄ derivative recorded in the same solvent. The results are summarized in Table 2, and typical ¹H NMR spectra are depicted in Figure 5.

Table 2. Proportion of Heteroleptic Complex Obtained upon Reaction of the Various PP Ligands with Cu(CH₃CN)₄BF₄ and dmp, dpep, or dpp as Deduced from Integration of the ¹H NMR Spectra of the Crude Product Mixture

	dmp	dpep	dpp
dppm	30%	10%	traces
dppe	80%	15%	traces
dppp	80%	10%	traces
dppb	65%	5%	traces
dppFc	>99%	>99%	traces
POP	>99.5%	>99.5%	traces

Whereas the heteroleptic [Cu(NN)(PP)]⁺ complexes were the only reaction products whatever the PP ligand when starting from 2,9-unsubstituted-1,10-phenanthrolines, the situation became completely different when 2,9-substituted-1,10-phenanthroline derivatives were used as starting material. Effectively, when using dmp and dpep as reagents, a mixture of [Cu(NN)(PP)]BF₄, [Cu(NN)₂]BF₄, and [Cu(PP)₂]BF₄ was always obtained and their relative proportion found to be highly dependent on the bis-phosphine ligand (Table 2). In contrast, homoleptic complexes were obtained as the only detectable products when dpp was used as the NN ligand. Obviously, steric effects resulting from the presence of the bulky phenyl rings on the dpp ligand destabilize the heteroleptic [Cu(dpp)(PP)]⁺ complexes. In addition to the remarkable thermodynamic stability of [Cu(dpp)₂]BF₄,²⁰ this negative steric effect drives the dynamic complexation scenario toward formation of homoleptic complexes almost exclusively.

dppFc and POP. [Cu(dmp)(dppFc)]BF₄,¹⁰ [Cu(dmp)(POP)]BF₄,^{3,4} [Cu(dpep)(dppFc)]BF₄,¹⁰ and [Cu(dpep)(POP)]BF₄⁸ were obtained pure by vapor diffusion of Et₂O into a CH₂Cl₂ solution of the corresponding reaction mixture. The four compounds have been already reported in the literature, and X-ray crystal structures of three of them are

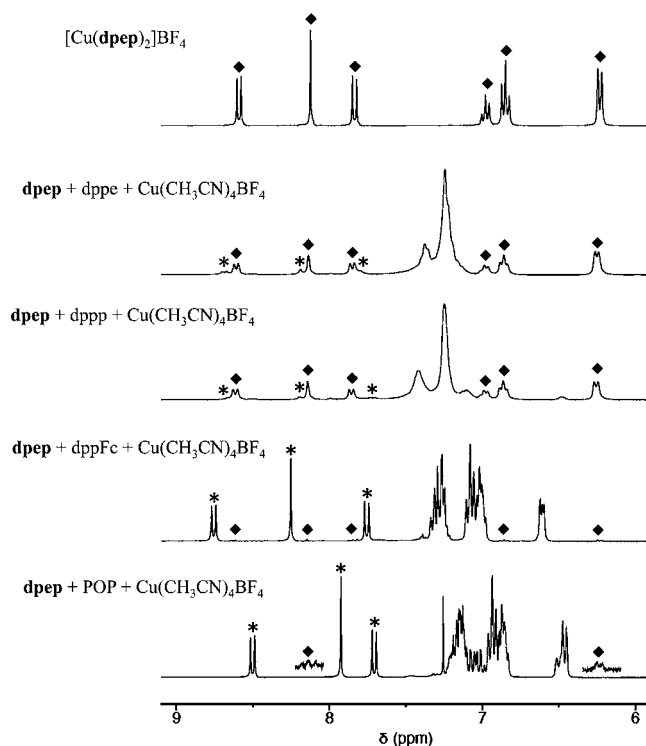


Figure 5. Aromatic region of the ¹H NMR spectra of the crude products obtained after treatment of various PP ligands with Cu(CH₃CN)₄BF₄ and dpep: (◆) [Cu(dpep)₂]BF₄; (*) [Cu(dpep)(PP)]BF₄. For comparison purposes, the ¹H NMR spectrum of [Cu(dpep)₂]BF₄ (top) is also represented.

known. Values of 113.18°, 116.44°, and 117.98° have been reported for the P-Cu-P bond angles of [Cu(dmp)(dppFc)]BF₄,¹⁰ [Cu(dmp)(POP)]BF₄,^{3,4} and [Cu(dpep)(POP)]BF₄,⁸ respectively. ¹H and ³¹P NMR analysis of the recrystallized samples recorded in CD₂Cl₂ revealed that the heteroleptic complex was the largely major species present in solution (>99%). However, traces of [Cu(dmp)₂]BF₄²¹ or [Cu(dpep)₂]BF₄¹⁵ were always detected in the ¹H NMR, thus showing that ligand exchange reactions take place to a minor extent for the heteroleptic complexes prepared from 2,9-disubstituted-1,10-phenanthroline and dppFc or POP.

dppm, dppe, dppp, and dppb. Some of the heteroleptic complexes were obtained pure as crystalline solids by vapor diffusion of Et₂O into a CH₂Cl₂ solution of the corresponding reaction mixture. This was the case for [Cu₂(dmp)₂(μ-dppm)₂](BF₄)₂, [Cu(dmp)(dppe)]BF₄, [Cu(dmp)(dppp)]BF₄, and [Cu(dmp)(dppb)]BF₄. All attempts to obtain other heteroleptic complexes in a pure form by recrystallization of the crude product mixture failed. Indeed, slow diffusion of Et₂O into a CH₂Cl₂ solution of the mixture of complexes yielded either only orange-red crystals of [Cu(NN)₂]BF₄ or a mixture of orange-red and yellow crystals corresponding to [Cu(NN)₂]BF₄ and [Cu(NN)(PP)]BF₄, respectively.

X-ray-quality crystals were obtained for both [Cu(dmp)(dppe)]BF₄ and [Cu(dmp)(dppp)]BF₄. Their X-ray crystal structures are depicted in Figure 6. Selected bond lengths and angles are summarized in Table 3.

Structures of the [Cu(dmp)(dppe)]⁺ and [Cu(dmp)(dppp)]⁺ cations are similar to the one described for the X-ray crystal structures of the corresponding PF₆⁻ salts.⁵ Whereas no particular differences in bond lengths are observed for

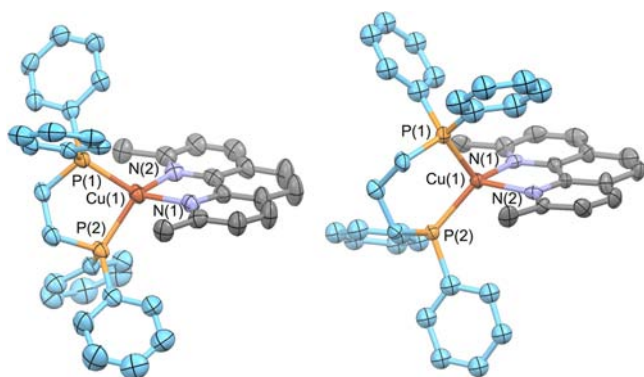


Figure 6. Structures of $[\text{Cu}(\text{dmp})(\text{dppe})]\text{BF}_4 \cdot \text{Et}_2\text{O}$ (left) and $[\text{Cu}(\text{dmp})(\text{dppp})]\text{BF}_4$ (right). H atoms, solvent in the case of dppe, and counteranion are omitted for clarity; thermal ellipsoids are drawn at the 50% probability level.

Table 3. Bond Distances and Bond Angles within the Coordination Sphere of $[\text{Cu}(\text{dmp})(\text{PP})]\text{BF}_4$ (PP = dppe and dppp, see Figure 6 for the numbering)

	selected bond lengths (Å)		selected bond angles (deg)		
	PP = dppe	PP = dppp	PP = dppe	PP = dppp	
Cu(1)–P(1)	2.267(2)	2.268(3)	P(1)–Cu(1)–P(2)	91.54(7)	104.2(1)
Cu(1)–P(2)	2.273(2)	2.261(3)	P(1)–Cu(1)–N(1)	132.1(2)	121.9(2)
Cu(1)–N(1)	2.059(6)	2.091(8)	P(1)–Cu(1)–N(2)	119.7(2)	108.0(2)
Cu(1)–N(2)	2.050(6)	2.090(8)	P(2)–Cu(1)–N(1)	114.5(2)	120.7(2)
			P(2)–Cu(1)–N(2)	120.3(2)	119.5(2)
			N(1)–Cu(1)–N(2)	82.2(2)	81.3(3)

$[\text{Cu}(\text{dmp})(\text{dppe})]\text{BF}_4$ and $[\text{Cu}(\text{dmp})(\text{dppp})]\text{BF}_4$, the bond angles around the Cu(I) cation are significantly different as a

result of the P–Cu–P angles imposed by the different number of methylene units between the two P atoms in both complexes. It can be noted that the PPh_2 groups do not significantly interact with the dmp ligand; however, in both cases, they are sterically close to the methyl groups which are located in between two phenyl groups. The closest C–H (Me) to phenyl distances ranges from 2.54 to 2.85 Å for $[\text{Cu}(\text{dmp})(\text{dppe})]\text{BF}_4$. Values ranging from 2.85 to 3.30 Å are seen for $[\text{Cu}(\text{dmp})(\text{dppp})]\text{BF}_4$. These observations explain well the observed destabilization of heteroleptic complexes prepared from 2,9-disubstituted-1,10-phenanthroline ligands (vide infra).

Whereas all dmp-containing heteroleptic complexes obtained in pure form by recrystallization were perfectly stable in the solid state, it is important to highlight that equilibration between the homoleptic and the heteroleptic complexes was observed as soon as the crystals are dissolved (even in a noncoordinating solvent such as CH_2Cl_2). Indeed, the heteroleptic/homoleptic ratio deduced from the ^1H NMR spectrum is exactly the same as the one observed in the crude mixture (Table 2). These observations show that ligand exchange reactions are taking place in solution for all compounds. In other words, there is a dynamic equilibrium between the heteroleptic complexes and the corresponding homoleptic species in solution (Figure 7). Indeed, all species present in the solutions were clearly identified by ^1H and ^{31}P NMR spectroscopy as well as by FAB mass spectrometry.

Typical resonances of both $[\text{Cu}(\text{dmp})(\text{PP})]^+$ and $[\text{Cu}(\text{dmp})_2]^+$ derivatives were clearly recognized in the ^1H NMR spectra of the dynamic mixtures, but typical resonances of $[\text{Cu}(\text{PP})_2]\text{BF}_4$ were not always easily distinguishable (Figure 8). The presence of the homoleptic complex $[\text{Cu}(\text{PP})_2]\text{BF}_4$ was however unambiguously demonstrated by ^{31}P NMR spectroscopy (Figure 9). $[\text{Cu}(\text{dppm})_2]\text{BF}_4$,¹¹ $[\text{Cu}(\text{dppe})_2]\text{BF}_4$,²² $[\text{Cu}(\text{dppp})_2]\text{BF}_4$,²² and $[\text{Cu}(\text{dppb})_2]\text{BF}_4$ ¹¹ are all known compounds, and their ^{31}P NMR spectra are described in the literature. For all systems the diagnostic signals of both homoleptic and heteroleptic complexes were clearly observed at

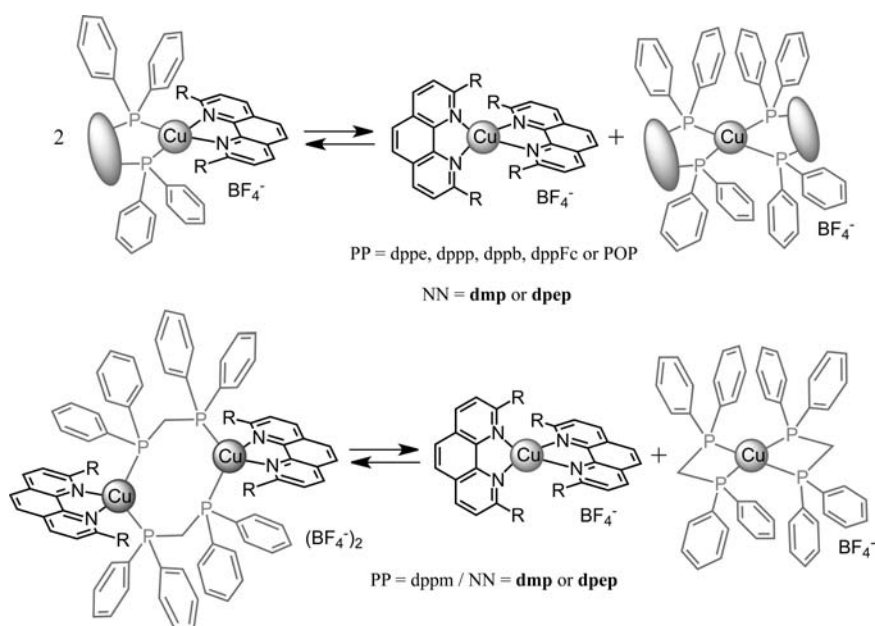


Figure 7. Dynamic equilibrium evidenced in solution between the heteroleptic complexes and their corresponding homoleptic species.

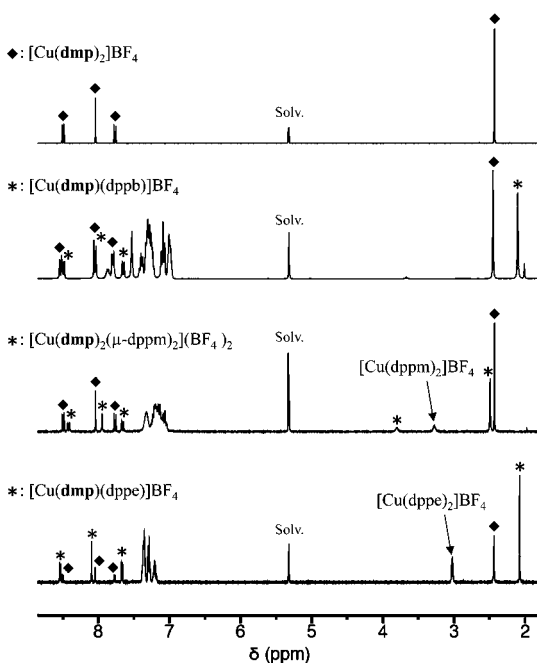


Figure 8. ^1H NMR (CD_2Cl_2) recorded upon dissolution of recrystallized samples of $[\text{Cu}_2(\text{dmp})_2(\mu\text{-dppm})_2](\text{BF}_4)_2$, $[\text{Cu}(\text{dmp})(\text{dppe})]\text{BF}_4$, and $[\text{Cu}(\text{dmp})(\text{dppb})]\text{BF}_4$. In all cases, ligand exchange reactions take place and the typical resonances of $[\text{Cu}(\text{dmp})_2]\text{BF}_4$ are clearly observed. For comparison purposes, the ^1H NMR spectrum of $[\text{Cu}(\text{dmp})_2]\text{BF}_4$ (top) is also represented.

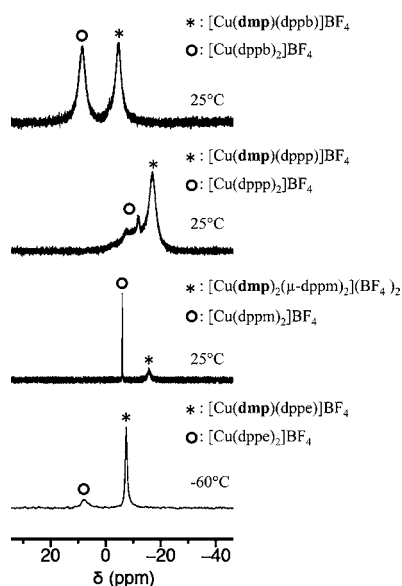


Figure 9. $^{31}\text{P}\{^1\text{H}\}$ NMR (CD_2Cl_2) recorded upon dissolution of recrystallized samples of $[\text{Cu}(\text{dmp})(\text{dppb})]\text{BF}_4$, $[\text{Cu}(\text{dmp})(\text{dppe})]\text{BF}_4$, $[\text{Cu}_2(\text{dmp})_2(\mu\text{-dppm})_2](\text{BF}_4)_2$, and $[\text{Cu}(\text{dmp})(\text{dppe})]\text{BF}_4$. In all cases, ligand exchange reactions take place and the typical resonances of $[\text{Cu}(\text{PP})_2]\text{BF}_4$ are clearly observed.

room temperature (Figure 9) except in the case of dppe. Actually, the ^{31}P NMR signal of $[\text{Cu}(\text{dppe})_2]\text{BF}_4$ is particularly broad at room temperature,²² preventing its observation under these conditions. As reported in the literature, lowering the temperature led to a significant decrease of $\Delta\nu_{1/2}$, and the characteristic signal observed at $\delta = +7.8$ ppm confirmed the presence of $[\text{Cu}(\text{dppe})_2]\text{BF}_4$ in solution.

It can also be noted that the ^{31}P NMR resonance of $[\text{Cu}(\text{dppp})_2]\text{BF}_4$ is not well resolved and appears complicated at room temperature. Detailed variable-temperature NMR studies have been reported for this compound²² and the complicated ^{31}P NMR pattern of $[\text{Cu}(\text{dppp})_2](\text{BF}_4)$ explained by a slow conformational exchange (ring inversion) on the NMR time scale. Indeed, at low temperature the phosphorus atoms of $[\text{Cu}(\text{dppp})_2]\text{BF}_4$ are nonequivalent as a result of a frozen chair conformation of the CuP_2C_3 six-membered rings.

It is well known that thermodynamically stable copper(I) complexes are also kinetically labile, and fast ligand exchange is often observed in solution at ambient temperature.²³ This is also clearly observed for the Cu(I) complexes prepared from bis-phosphines and phenanthroline ligands. In this particular case, whatever the ratio of homoleptic and heteroleptic complexes in solution, all ligands and metal binding sites are utilized to generate coordinatively saturated complexes. Therefore, the equilibrium between the different complexes must be mainly governed by the relative thermodynamic stability of the different possible complexes.²⁴ On one hand, homoleptic $[\text{Cu}(\text{NN})_2]^+$ complexes prepared from 2,9-disubstituted-1,10-phenanthroline ligands are particularly stable ($\log \beta = 10\text{--}12$);²⁰ they have thus a priori tendency to drive the equilibrium toward formation of the homoleptic complexes. In contrast, this is not the case for the Cu(I) complexes obtained from 2,9-unsubstituted-1,10-phenanthrolines. The corresponding $[\text{Cu}(\text{NN})_2]^+$ complexes are actually less stable and therefore unable to significantly compete with formation of $[\text{Cu}(\text{NN})(\text{PP})]^+$. On the other hand, subtle steric effects may also contribute to stabilize/destabilize both $[\text{Cu}(\text{PP})_2]^+$ and $[\text{Cu}(\text{NN})(\text{PP})]^+$ derivatives. Actually, the differences in behavior observed for the various bis-phosphine ligands may be explained by the differences in bite angles for the different chelating P ligands. When this angle is small enough (dppe, dppp, and dppb), the Cu(I) center can easily accommodate two ligands to form a stable homoleptic complex.^{11,22} In contrast, steric factors resulting from the wider P–Cu–P angle for the other bis-phosphines (dppFc and POP) may substantially destabilize the $[\text{Cu}(\text{PP})_2]^+$ derivative. This is clearly seen in the case of $[\text{Cu}(\text{POP})_2]^+$ for which a X-ray crystal structure could be obtained (Figure 10).²⁵ The Cu(I) cation is effectively too small to accommodate two POP ligands in a tetrahedral coordination geometry. Only one POP ligand is chelating the metal, while the other one is acting as a monodentate ligand. As a result the Cu(I) cation is in a distorted trigonal coordination geometry.

The homoleptic Cu(I) complex prepared from dppFc has been characterized in solution by Long and co-workers, but no X-ray crystal structure has been published for this compound.²⁶ We decided to prepare this compound from dppFc and $\text{Cu}(\text{CH}_3\text{CN})_4\text{BF}_4$. As reported by Long and co-workers, the resulting complex displays broadened ^1H and ^{31}P NMR features at room temperature, suggesting dissociative processes in solution. Crystals were obtained by slow diffusion of Et_2O into a CH_2Cl_2 solution of the crude mixture of complexes. Surprisingly, their X-ray crystal structure analysis revealed formation of a dinuclear Cu(I) complex (Figure 10). Each metal center is chelated by a dppFc ligand, and the two $[\text{Cu}(\text{dppFc})]^+$ subunits are connected by an additional bridging dppFc ligand. ^1H and ^{31}P NMR spectra recorded upon dissolution of the recrystallized sample are different when compared to the crude mixture. This is consistent with a different ligand to metal ratio in solution. However, as in the

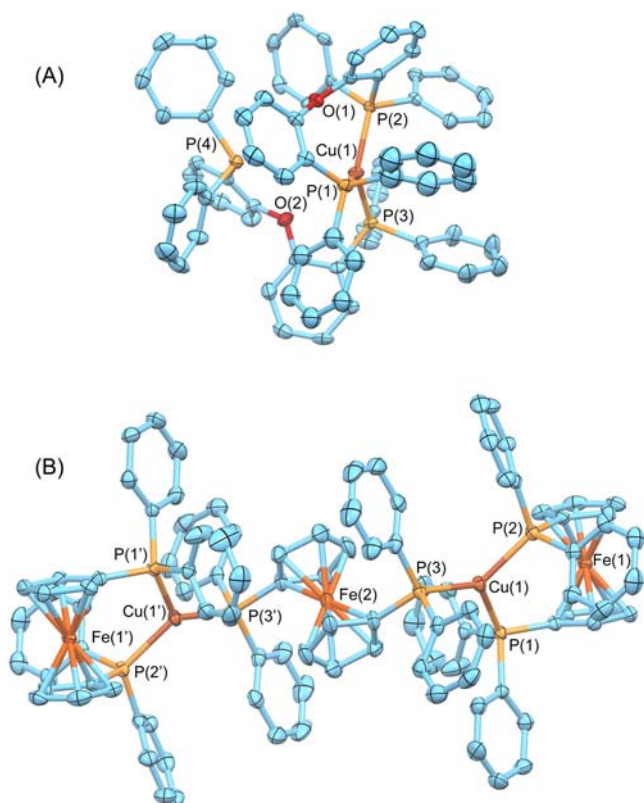


Figure 10. (A) Structure of $[\text{Cu}(\text{POP})_2]\text{BF}_4$. H atoms and counteranion are omitted for clarity; thermal ellipsoids are drawn at the 50% probability level. Selected bond lengths (Angstroms): $\text{Cu}(1)\text{--P}(1)$ 2.273(1), $\text{Cu}(1)\text{--P}(2)$ 2.261(1), $\text{Cu}(1)\text{--P}(3)$ 2.263(1). Selected bond angles (degrees): $\text{P}(1)\text{--Cu}(1)\text{--P}(2)$ 114.03(6), $\text{P}(1)\text{--Cu}(1)\text{--P}(3)$ 121.49(6), $\text{P}(2)\text{--Cu}(1)\text{--P}(3)$ 121.90(6). $\text{P}(4)$ is at a nonbonding distance from the Cu center (3.96 Å). (B) Structure of $[\text{Cu}_2(\text{dppFc})_3](\text{BF}_4)_2 \cdot (\text{H}_2\text{O})_2 \cdot \text{CH}_2\text{Cl}_2$. H atoms, solvent molecules, and counteranions are omitted for clarity; thermal ellipsoids are drawn at the 50% probability level. Selected bond lengths (Angstroms): $\text{Cu}(1)\text{--P}(1)$ 2.264(2), $\text{Cu}(1)\text{--P}(2)$ 2.273(1), $\text{Cu}(1)\text{--P}(3)$ 2.248(2). Selected bond angles (degrees): $\text{P}(1)\text{--Cu}(1)\text{--P}(2)$ 111.72(6), $\text{P}(1)\text{--Cu}(1)\text{--P}(3)$ 122.47(7), $\text{P}(2)\text{--Cu}(1)\text{--P}(3)$ 125.01(7).

case of the crude mixture, NMR data suggest the presence of several species in solution. Being out of the scope of the present investigation, this system was not further investigated.

X-ray crystal structure analysis of the homoleptic Cu(I) complexes prepared from dppFc and POP revealed that the Cu(I) cation is too small to accommodate two ligands in a distorted tetrahedral coordination geometry. Indeed, the large P–Cu–P angle prevents formation of a tetracoordinated complex in both cases. As mentioned above, these homoleptic complexes are thus destabilized, and this effect contributes to favor formation of the $[\text{Cu}(\text{NN})(\text{PP})]^+$ derivatives.

Finally, the difference in bite angle for the various chelating P ligands may also affect the stability of $[\text{Cu}(\text{NN})(\text{PP})]^+$. Indeed, when the phenanthroline ligand is substituted in its 2 and 9 positions, negative steric effects may contribute to destabilize the heteroleptic complex. This view is indeed supported by the X-ray crystal structures of $[\text{Cu}(\text{dmp})(\text{dppe})]\text{BF}_4$ and $[\text{Cu}(\text{dmp})(\text{dppp})]\text{BF}_4$ in which the methyl groups of the dmp ligand are close to the phenyl units of the PPh_2 moieties. In the case of dppb, the P–Cu–P angle is in the same range and similar steric effects are expected. These observations explain

also well the further destabilization observed for the corresponding heteroleptic complexes prepared from dpep. Steric hindrance may also limit the stability of the dinuclear Cu(I) complexes obtained from dppm and 2,9-disubstituted-1,10-phenanthrolines. For all these P ligands, steric effects are involved in destabilization of the heteroleptic complexes and thus contribute, at least in part, to displacing the dynamic mixture toward the homoleptic species. In contrast, for dppFc and POP, the P–Cu–P angle is wider (113–118°) and the wrapping of the phenanthroline ligand is more effective in $[\text{Cu}(\text{NN})(\text{PP})]^+$. As a result, the orientation of the phenyl groups of the two PPh_2 subunits is different and negative steric effects are limited. In addition to destabilization of the homoleptic Cu(I) complexes of dppFc and POP (vide supra), this limited steric hindrance drives the system toward almost exclusive formation of the heteroleptic complexes.

CONCLUSIONS

The systematic investigations done with the libraries of phenanthroline derivatives and bis-phosphine ligands shown in Chart 1 revealed several important trends: (i) whatever the bis-phosphine ligand, stable heteroleptic complexes are obtained from 1,10-phenanthroline; (ii) 4,7-substituents on the phenanthroline ligand (Bphen) have no negative influence on formation of the heteroleptic complexes; (iii) heteroleptic complexes obtained from dmp are stable in the solid state, but a dynamic ligand exchange reaction is systematically observed in solution, and the homoleptic/heteroleptic ratio is highly dependent on the bis-phosphine ligand; (iv) by increasing the size of the 2,9-substituents, e.g., when going from dmp to dpep, the heteroleptic complexes are further destabilized and the homoleptic complexes are favored except in the cases of dppFc and POP for which the heteroleptic complexes are still almost exclusively obtained, (v) by further increasing the size of the 2,9-substituents, e.g., when going from dpep to dpp, only homoleptic complexes were obtained whatever the bis-phosphine ligand as a result of steric hindrance, (vi) the difference in behavior of the various bis-phosphine ligands has been explained by their different chelate bite angles influencing the stability of both $[\text{Cu}(\text{NN})(\text{PP})]^+$ and $[\text{Cu}(\text{PP})_2]^+$; the remarkable stability of the dppFc- and POP-containing heteroleptic derivatives results from a substantial destabilization of both $[\text{Cu}(\text{dppFc})_2]^+$ and $[\text{Cu}(\text{POP})_2]^+$ species as well as from a favorable orientation of the aromatic groups of the PPh_2 moieties limiting steric hindrance effects when the phenanthroline ligand is substituted in its 2 and 9 positions.

Detailed analysis revealed that the dynamic equilibrium resulting from ligand exchange reactions is mainly influenced by the relative thermodynamic stability of the different possible complexes. The exceptionally high thermodynamic stability of the homoleptic $[\text{Cu}(\text{NN})_2]^+$ complexes tends to drive the equilibrium toward formation of the homoleptic complexes; this is particularly the case when steric hindrance effects destabilize the $[\text{Cu}(\text{NN})(\text{PP})]^+$ derivatives prepared from 2,9-disubstituted-1,10-phenanthroline ligands. This effect is however in part counterbalanced by a substantial destabilization of the $[\text{Cu}(\text{PP})_2]^+$ derivatives in the case of POP and dppFc. With these particular chelating P ligands, stable $[\text{Cu}(\text{NN})(\text{PP})]^+$ derivatives are obtained even from 1,10-phenanthroline ligands bearing substituents of a reasonable size at the 2,9-positions.

Most of the copper(I) complexes described in the present paper show interesting electronic properties which have been

already investigated in detail. The results will be described in a second paper.

EXPERIMENTAL SECTION

General Procedures. Reagents were purchased as reagent grade and used without further purification. Compounds dpep,¹⁵ dpp,¹⁴ [Cu(dpep)₂]BF₄¹⁵ and [Cu(dmp)₂]BF₄²¹ were prepared according to previously reported procedures. Acetonitrile (CH₃CN) was distilled over CaH₂ under Ar. Dichloromethane (CH₂Cl₂) was distilled over CaH₂ under Ar. All reactions were performed in standard glassware under an inert Ar atmosphere. Evaporation and concentration were done at water aspirator pressure and drying in vacuo at 10⁻² Torr. Column chromatography: silica gel 60 (230–400 mesh, 0.040–0.063 mm) was purchased from E. Merck. Thin layer chromatography (TLC) was performed on aluminum sheets coated with silica gel 60 F₂₅₄ purchased from E. Merck. NMR spectra were recorded on a Bruker AC 300 or AC 400 with solvent peaks as reference. Elemental analyses were carried out on a Perkin-Elmer 2400 B analyzer at the LCC Microanalytical Laboratory in Toulouse. Mass spectra were obtained at the Service Commun de Spectrométrie de Masse de l'Université Paul Sabatier et du CNRS de Toulouse. Fast atom bombardment (FAB) spectra were performed on a Nermag R 10–10H spectrometer. A 9 kV xenon atom beam was used to desorb samples from the 3-nitrobenzyl alcohol matrix.

General Procedure for Preparation of [Cu(phen)(PP)]BF₄ and [Cu(Bphen)(PP)]BF₄. A solution of the appropriate bis-phosphine ligand (1 equiv) and Cu(CH₃CN)₄BF₄ (1 equiv) in a 7:3 CH₂Cl₂/CH₃CN mixture was stirred for 0.5 h; then phen or Bphen (1 equiv) was added. After 1 h, solvents were evaporated. Heteroleptic complexes were then obtained pure as crystalline solids by slow diffusion of Et₂O into a CH₂Cl₂ solution of the crude product.

[Cu(phen)(dpep)]BF₄. This compound was thus obtained in 86% yield as a yellow crystalline solid. ¹H NMR (CD₂Cl₂, 300 MHz, 293 K): 8.76 (d, *J* = 4 Hz, 2H), 8.67 (d, *J* = 8 Hz, 2H), 8.17 (s, 2H), 7.90 (dd, *J* = 8 Hz, *J* = 4 Hz, 2H), 7.39 (m, 20H), 2.76 (t, *J* = 6 Hz, 4H). ³¹P{¹H} NMR (CD₂Cl₂, 293 K, 162 MHz): –4.80. ¹³C{¹H} NMR (CD₂Cl₂, 298 K, 75 MHz): 150.9, 144.7, 138.6, 133.1, 132.9 (t, *J*_{P–C} = 8 Hz), 132.8, 132.6, 131.4, 130.7, 130.1 (t, *J*_{P–C} = 4 Hz), 128.2, 125.9, 26.4 (t, *J*_{P–C} = 19 Hz). Anal. Calcd for C₃₈H₃₂N₂P₂CuBF₄: C, 62.61; H, 4.42; N, 3.84. Found: C, 62.72; H, 4.56; N, 3.80. FAB-MS: 641.0 ([M – BF₄]⁺, calcd for C₃₈H₃₂N₂P₂Cu 641.13).

[Cu(phen)(dppp)]BF₄. This compound was thus obtained in 62% yield as a yellow crystalline solid. ¹H NMR (CD₂Cl₂, 300 MHz, 293 K): 8.77 (d, *J* = 4 Hz, 2H), 8.60 (d, *J* = 8 Hz, 2H), 8.12 (s, 2H), 7.83 (dd, *J* = 8 Hz, *J* = 4 Hz, 2H), 7.36 (m, 4H), 7.24 (m, 16H), 2.71 (m, 4H), 2.34 (m, 2H). ³¹P{¹H} NMR (CD₂Cl₂, 293 K, 162 MHz): –13.39. ¹³C{¹H} NMR (CD₂Cl₂, 298 K, 75 MHz): 150.8, 144.4, 138.3, 134.2 (t, *J*_{P–C} = 16 Hz, 4C), 132.7 (t, *J*_{P–C} = 8 Hz), 130.9, 130.6, 129.7 (t, *J*_{P–C} = 5 Hz), 128.2, 125.8, 29.5 (t, *J*_{P–C} = 8 Hz), 20.6 (t, *J*_{P–C} = 4 Hz). Anal. Calcd for C₃₉H₃₄N₂P₂CuBF₄·CH₂Cl₂: C, 58.03; H, 4.38; N, 3.38. Found: C, 57.94; H, 4.75; N, 3.11. FAB-MS: 655 ([M – BF₄]⁺, calcd for C₃₉H₃₄N₂P₂Cu 655.15).

[Cu(phen)(dppb)]BF₄. This compound was thus obtained in 93% yield as a yellow crystalline solid. ¹H NMR (CD₂Cl₂, 300 MHz, 293 K): 8.59 (d, *J* = 8 Hz, 2H), 8.35 (d, *J* = 4 Hz, 2H), 8.09 (s, 2H), 7.79 (dd, *J* = 8 Hz, *J* = 5 Hz, 2H), 7.66 (m, 4H), 7.44 (m, 4H), 7.35 (m, 8H), 7.25 (m, 8H). ³¹P{¹H} NMR (CD₂Cl₂, 293 K, 162 MHz): –2.94. ¹³C{¹H} NMR (CD₂Cl₂, 298 K, 75 MHz): 150.7, 144.6, 142.0, 138.5, 135.7 (t, *J*_{P–C} = 4 Hz), 133.5 (t, *J*_{P–C} = 8 Hz), 133.1, 132.9, 132.6, 132.3, 131.1, 130.5, 129.9 (t, *J*_{P–C} = 5 Hz), 128.1, 125.8. Anal. Calcd for C₄₂H₃₂N₂P₂CuBF₄: C, 59.92; H, 3.97; N, 3.25. Found: C, 60.01; H, 3.99; N, 3.01. FAB-MS: 689 ([M – BF₄]⁺, calcd for C₄₂H₃₂N₂P₂Cu 689.13).

[Cu(phen)(dppf)]BF₄. This compound was thus obtained in 75% yield as an orange crystalline solid. Analytical data were identical to those described in the literature.¹⁰

[Cu(phen)(POP)]BF₄. This compound was thus obtained in 95% yield as a yellow crystalline solid. Analytical data were identical to those described in the literature.^{3,4}

[Cu₂(phen)₂(μ-dppm)₂](BF₄)₂. This compound was thus obtained in 87% yield as a yellow crystalline solid. ¹H NMR (CD₂Cl₂, 300 MHz, 293 K): 8.68 (d, *J* = 4 Hz, 4H), 8.24 (d, *J* = 8 Hz, 4H), 7.77 (m, 4H), 7.69 (s, 4H), 7.07–6.87 (m, 40H), 3.88 (m, 4H). ³¹P{¹H} NMR (CD₂Cl₂, 293 K, 162 MHz): –6.62. Anal. Calcd for C₇₄H₆₀N₄P₄Cu₂B₂F₈: C, 62.16; H, 4.23; N, 3.92. Found: C, 62.43; H, 4.55; N, 3.92.

[Cu(Bphen)(dppe)]BF₄. This compound was thus obtained in 61% yield as a yellow crystalline solid. ¹H NMR (CD₂Cl₂, 300 MHz, 293 K): 8.86 (d, *J* = 5 Hz, 2H), 8.19 (s, 2H), 7.87 (d, *J* = 5 Hz, 2H), 7.68 (m, 10H), 7.53–7.41 (m, 20H), 2.83 (t, *J* = 6 Hz, 4H). ³¹P{¹H} NMR (CD₂Cl₂, 293 K, 162 MHz): –4.44. ¹³C{¹H} NMR (CD₂Cl₂, 298 K, 75 MHz): 151.2, 150.5, 145.4 (t, *J*_{P–C} = 2 Hz), 137.0, 133.0 (t, *J*_{P–C} = 8 Hz), 132.9, 132.7, 131.4, 130.4, 130.3, 130.1 (t, *J*_{P–C} = 5 Hz), 129.8, 128.5, 126.1, 125.9, 26.4 (t, *J*_{P–C} = 19 Hz). Anal. Calcd for C₅₀H₄₀N₂P₂CuBF₄: C, 68.15; H, 4.57; N, 3.18. Found: C, 68.32; H, 4.35; N, 3.34. FAB-MS: 793 ([M – BF₄]⁺, calcd for C₅₀H₄₀N₂P₂Cu 793.2).

[Cu(Bphen)(dppp)]BF₄. This compound was thus obtained in 65% yield as a yellow crystalline solid. ¹H NMR (CD₂Cl₂, 300 MHz, 293 K): 8.84 (d, *J* = 5 Hz, 2H), 8.12 (s, 2H), 7.77 (d, *J* = 5 Hz, 2H), 7.63 (m, 10H), 7.41–7.29 (m, 20H), 2.77 (m, 4H), 2.38 (m, 2H). ³¹P{¹H} NMR (CD₂Cl₂, 293 K, 162 MHz): –13.03. ¹³C{¹H} NMR (CD₂Cl₂, 298 K, 75 MHz): 150.9, 150.4, 145.1 (t, *J*_{P–C} = 2 Hz), 137.0, 134.3 (t, *J*_{P–C} = 16 Hz), 132.8 (t, *J*_{P–C} = 8 Hz), 130.9, 130.4, 130.3, 129.8, 129.7, 129.73, 129.6, 128.4, 126, 125.8, 29.5 (t, *J*_{P–C} = 8 Hz), 20.6 (t, *J*_{P–C} = 2 Hz). Anal. Calcd for C₅₁H₄₂N₂P₂CuBF₄: C, 68.43; H, 4.73; N, 3.13. Found: C, 68.12; H, 4.90; N, 2.99. FAB-MS: 807 ([M – BF₄]⁺, calcd for C₅₁H₄₂N₂P₂Cu 807.21).

[Cu(Bphen)(dppb)]BF₄. This compound was thus obtained in 90% yield as a yellow crystalline solid. ¹H NMR (CD₂Cl₂, 300 MHz, 293 K): 8.44 (d, *J* = 5 Hz, 2H), 8.11 (s, 2H), 7.76 (d, *J* = 5 Hz, 2H), 7.70 (m, 4H), 7.63 (m, 10H), 7.49–7.29 (m, 20H). ³¹P{¹H} NMR (CD₂Cl₂, 293 K, 162 MHz): –2.71. ¹³C{¹H} NMR (CD₂Cl₂, 298 K, 75 MHz): 151.1, 150.2, 145.2 (t, *J*_{P–C} = 2 Hz), 142.1 (t, *J*_{P–C} = 35 Hz), 136.9, 135.7 (t, *J*_{P–C} = 4 Hz), 133.5 (t, *J*_{P–C} = 8 Hz), 133.2, 132.9, 132.7, 132.4, 131.1, 130.4, 130.3, 129.9, 129.92, 129.8, 129.81, 128.3, 126.0, 125.8. Anal. Calcd for C₅₄H₄₀N₂P₂CuBF₄·H₂O: C, 68.47; H, 4.47; N, 2.96. Found: C, 68.12; H, 4.71; N, 3.07. FAB-MS: 841 ([M – BF₄]⁺, calcd for C₅₄H₄₀N₂P₂Cu 841.2).

[Cu(Bphen)(dppf)]BF₄. This compound was thus obtained in 70% yield as an orange crystalline solid. ¹H NMR (CD₂Cl₂, 300 MHz, 293 K): 8.83 (d, *J* = 5 Hz, 2H), 8.09 (s, 2H), 7.67–7.58 (m, 12H), 7.33 (m, 20H), 4.59 (m, 4H), 4.45 (m, 4H). ³¹P{¹H} NMR (CD₂Cl₂, 293 K, 162 MHz): –8.70. ¹³C{¹H} NMR (CD₂Cl₂, 298 K, 100 MHz): 150.9, 150.4, 144.8 (t, *J*_{P–C} = 2 Hz), 137.0, 134.4, 134.1, 133.9, 133.8 (t, *J*_{P–C} = 8 Hz), 131, 130.4, 130.3, 129.8, 129.5 (t, *J*_{P–C} = 5 Hz), 128.4, 126.0, 125.8, 75.44, 75.4 (t, *J*_{P–C} = 5 Hz), 75.2, 74.9, 73.7 (t, *J*_{P–C} = 2 Hz). Anal. Calcd for C₅₈H₄₄N₂P₂FeCuBF₄: C, 67.17; H, 4.28; N, 2.70. Found: C, 67.05; H, 4.44; N, 2.67. FAB-MS: 949 ([M – BF₄]⁺, calcd for C₅₈H₄₄N₂P₂FeCu 949.16).

[Cu(Bphen)(POP)]BF₄. This compound was thus obtained in 92% yield as a yellow crystalline solid. Analytical data were identical to those described in the literature.²⁶

[Cu₂(Bphen)₂(μ-dppm)₂](BF₄)₂. This compound was thus obtained in 48% yield as a yellow crystalline solid. ¹H NMR (CD₂Cl₂, 300 MHz, 293 K): 8.75 (d, *J* = 5 Hz, 4H), 7.72 (m, 8H), 7.58 (m, 13H), 7.51 (m, 7H), 7.09 (m, 25H), 6.96 (m, 15H), 3.98 (m, 4H). ³¹P{¹H} NMR (CD₂Cl₂, 293 K, 162 MHz): –6.45. ¹³C{³¹P}{¹H} NMR (CD₂Cl₂, 298 K, 75 MHz): 151.1, 150.1, 144.2, 137.3, 133.7, 133.3, 130.5, 130.4, 129.9, 129.7, 129.1, 127.5, 126.2, 124.9, 66.5, 27.3, 15.9. Anal. Calcd for C₉₈H₇₆N₄P₄Cu₂B₂F₈·CH₂Cl₂: C, 65.36; H, 4.32; N, 3.08. Found: C, 65.20; H, 4.01; N, 3.25. FAB-MS: 1647 ([M – BF₄]⁺, 10%, calcd for C₉₈H₇₆N₄P₄Cu₂B₂F₈ 1646.37), 780 ([M – (BF₄)₂]²⁺, 100%, calcd for C₉₈H₇₆N₄P₄Cu₂ 780.18).

General Procedure for Preparation of [Cu(dmp)(PP)]BF₄ and [Cu(dpep)(PP)]BF₄. A solution of the appropriate bis-phosphine ligand (1 equiv) and Cu(CH₃CN)₄BF₄ (1 equiv) in a 7:3 CH₂Cl₂/CH₃CN mixture was stirred for 0.5 h; then dmp or dpep (1 equiv) was added. After 1 h, solvents were evaporated. Products were analyzed as

received by ^1H NMR. The relative proportion of the different possible complexes, i.e., $[\text{Cu}(\text{NN})(\text{PP})]\text{BF}_4$, $[\text{Cu}(\text{NN})_2]\text{BF}_4$, and $[\text{Cu}(\text{NN})_2]\text{BF}_4$, was deduced from comparison with the ^1H NMR spectrum of the corresponding $[\text{Cu}(\text{NN})_2]\text{BF}_4$ derivative recorded in the same solvent. Some of the heteroleptic complexes were obtained pure as crystalline solids by vapor diffusion of Et_2O into a CH_2Cl_2 solution of the corresponding reaction mixture. This was the case for $[\text{Cu}_2(\text{dmp})_2(\mu\text{-dppm})_2](\text{BF}_4)_2$, $[\text{Cu}(\text{dmp})(\text{dppe})]\text{BF}_4$, $[\text{Cu}(\text{dmp})(\text{dppp})]\text{BF}_4$, $[\text{Cu}(\text{dmp})(\text{dppb})]\text{BF}_4$, $[\text{Cu}(\text{dmp})(\text{dppFc})]\text{BF}_4$, $[\text{Cu}(\text{dmp})(\text{POP})]\text{BF}_4$, $[\text{Cu}(\text{dpep})(\text{dppFc})]\text{BF}_4$, and $[\text{Cu}(\text{dpep})(\text{POP})]\text{BF}_4$. All attempts to obtain the other heteroleptic complexes in a pure form by recrystallization of the crude product mixture failed. Indeed, slow diffusion of Et_2O into a CH_2Cl_2 solution of the mixture of complexes yielded either only orange-red crystals of $[\text{Cu}(\text{NN})_2]\text{BF}_4$ or a mixture of orange-red and yellow crystals corresponding to $[\text{Cu}(\text{NN})_2]\text{BF}_4$ and $[\text{Cu}(\text{NN})(\text{PP})]\text{BF}_4$, respectively.

$[\text{Cu}_2(\text{dmp})_2(\mu\text{-dppm})_2](\text{BF}_4)_2$. This compound was thus obtained in 52% yield as a yellow crystalline solid. As soon as dissolved in CH_2Cl_2 , ligand exchange took place and analysis of the ^1H NMR spectrum revealed the presence of different species in solution: $[\text{Cu}_2(\text{dmp})_2(\mu\text{-dppm})_2](\text{BF}_4)_2$, $[\text{Cu}(\text{dmp})_2]\text{BF}_4$,²¹ and $[\text{Cu}(\text{dppm})_2]\text{BF}_4$ in a 7:3:3 ratio.¹¹ The presence of $[\text{Cu}(\text{dppm})_2]\text{BF}_4$ was confirmed by its ^{31}P NMR resonance observed at $\delta = -6.03$ ppm; the additional peak observed in the ^{31}P NMR spectrum at $\delta = -15.67$ ppm is assigned to $[\text{Cu}_2(\text{dmp})_2(\mu\text{-dppm})_2](\text{BF}_4)_2$.

$[\text{Cu}(\text{dmp})(\text{dppe})]\text{BF}_4$. This compound was thus obtained in 69% yield as a yellow crystalline solid. As soon as dissolved in CH_2Cl_2 , ligand exchange took place and analysis of the ^1H NMR spectrum revealed the presence of different species in solution: $[\text{Cu}(\text{dmp})(\text{dppe})]\text{BF}_4$, $[\text{Cu}(\text{dmp})_2]\text{BF}_4$,²¹ and $[\text{Cu}(\text{dppe})_2]\text{BF}_4$ in a 4:1:1 ratio.²² The presence of $[\text{Cu}(\text{dppe})_2]\text{BF}_4$ was confirmed by its broad ^{31}P NMR resonance observed at $\delta = 7.80$ ppm (207 K); the additional peak observed in the ^{31}P NMR spectrum at $\delta = -7.53$ ppm is assigned to $[\text{Cu}(\text{dmp})(\text{dppe})]\text{BF}_4$. FAB-MS: 859.8 ($[\text{Cu}(\text{dppe})_2]^+$, 33%), 669.7 ($[\text{Cu}(\text{dppe})(\text{dmp})]^+$, 100%), 479.5 ($[\text{Cu}(\text{dmp})_2]^+$, 40%), 461.5 ($[\text{Cu}(\text{dppe})]^+$, 63%), 271.4 ($[\text{Cu}(\text{dmp})]^+$, 3%).

$[\text{Cu}(\text{dmp})(\text{dppp})]\text{BF}_4$. This compound was thus obtained in 76% yield as a yellow crystalline solid. As soon as dissolved in CH_2Cl_2 , ligand exchange took place and analysis of the ^1H NMR spectrum revealed the presence of different species in solution: $[\text{Cu}(\text{dmp})(\text{dppp})]\text{BF}_4$, $[\text{Cu}(\text{dmp})_2]\text{BF}_4$,²¹ and $[\text{Cu}(\text{dppp})_2]\text{BF}_4$ in a 4:1:1 ratio.²² The presence of $[\text{Cu}(\text{dppp})_2]\text{BF}_4$ was confirmed by its broad ^{31}P NMR resonance centered at $\delta = -10$ ppm; the additional peak observed in the ^{31}P NMR spectrum at $\delta = -17.01$ ppm is assigned to $[\text{Cu}(\text{dmp})(\text{dppp})]\text{BF}_4$.

$[\text{Cu}(\text{dmp})(\text{dppb})]\text{BF}_4$. This compound was thus obtained in 45% yield as a yellow crystalline solid. As soon as dissolved in CH_2Cl_2 , ligand exchange took place and analysis of the ^1H NMR spectrum revealed the presence of different species in solution: $[\text{Cu}(\text{dmp})(\text{dppb})]\text{BF}_4$, $[\text{Cu}(\text{dmp})_2]\text{BF}_4$,²¹ and $[\text{Cu}(\text{dppb})_2]\text{BF}_4$ in a 65:35:35 ratio.¹¹ The presence of $[\text{Cu}(\text{dppb})_2]\text{BF}_4$ was confirmed by its ^{31}P NMR resonance observed at $\delta = 8.42$ ppm; the additional peak observed in the ^{31}P NMR spectrum at $\delta = -4.64$ ppm is assigned to $[\text{Cu}(\text{dmp})(\text{dppb})]\text{BF}_4$.

$[\text{Cu}(\text{dmp})(\text{dppFc})]\text{BF}_4$. This compound was thus obtained in 90% yield as a yellow crystalline solid. Analytical data were identical to those described in the literature.¹⁰

$[\text{Cu}(\text{dmp})(\text{POP})]\text{BF}_4$. This compound was thus obtained in 70% yield as a yellow crystalline solid. Analytical data were identical to those described in the literature.^{3,4,10}

$[\text{Cu}(\text{dpep})(\text{dppFc})]\text{BF}_4$. This compound was thus obtained in 71% yield as a yellow crystalline solid. Analytical data were identical to those described in the literature.¹⁰

$[\text{Cu}(\text{dpep})(\text{POP})]\text{BF}_4$. This compound was thus obtained in 86% yield as a yellow crystalline solid. Analytical data were identical to those described in the literature.⁸

Preparation of $[\text{Cu}(\text{POP})_2]\text{BF}_4$. A mixture of $\text{Cu}(\text{CH}_3\text{CN})\text{BF}_4$ (0.05 g, 0.16 mmol) and POP (0.171 g, 0.32 mmol) in CH_2Cl_2 (10 mL) was stirred for 1 h at room temperature. The resulting solution was concentrated to ca. 5 mL. Crystals of $[\text{Cu}(\text{POP})_2]\text{BF}_4$ were

obtained by vapor diffusion of *n*-hexane into this CH_2Cl_2 solution. Compound $[\text{Cu}(\text{POP})_2]\text{BF}_4$ was thus obtained in 68% yield as colorless crystals. ^1H NMR (CD_2Cl_2 , 300 MHz, 293 K): 6.49 (d, $J = 4$ Hz, 2H), 6.76–6.83 (m, 10H), 7.00 (t, $J = 8$ Hz, 10H), 7.18 (td, $J = 8$ and 2 Hz, 2H), 7.26 (t, $J = 7$ Hz, 4H). $^{31}\text{P}\{^1\text{H}\}$ NMR (CD_2Cl_2 , 293 K, 121.5 MHz): -13.57. $^{13}\text{C}\{^{31}\text{P}\}\{^1\text{H}\}$ NMR (CD_2Cl_2 , 298 K, 75.5 MHz): 119.6, 125.0, 129.0, 130.5, 131.5, 132.4, 134.1, 134.7, 158.5. Anal. Calcd for $\text{C}_{72}\text{H}_{56}\text{O}_3\text{P}_4\text{CuBF}_4$: C, 70.45; H, 4.6. Found: C, 70.13; H, 4.44. FAB-MS: 1139.7 (17%, $[\text{Cu}(\text{POP})_2]^+$), 601.3 (100%, $[\text{Cu}(\text{POP})]^+$).

Preparation of the Homoleptic Complex from dppFc. A mixture of $\text{Cu}(\text{CNCH}_3)\text{BF}_4$ (0.03 g, 0.09 mmol) and DPPF (0.100 g, 0.18 mmol) in CH_2Cl_2 (10 mL) was stirred for 1 h at room temperature. The resulting solution was evaporated to yield an orange powder in quantitative yield. The product was analyzed as received. ^1H NMR (CD_2Cl_2 , 300 MHz, 298 K): 4.01 (br, 4H), 4.27 (br, 4H), 7.26–7.30 (m, 16H), 7.41–7.47 (m, 4H). $^{31}\text{P}\{^1\text{H}\}$ NMR (CD_2Cl_2 , 298 K, 121.5 MHz): -9.33. Anal. Calcd for $\text{C}_{68}\text{H}_{56}\text{P}_4\text{Fe}_2\text{CuBF}_4 \cdot 0.5\text{CH}_2\text{Cl}_2$: C, 63.21; H, 4.41. Found: C, 63.54; H, 3.99. As described in the literature for the corresponding PF_6 salt,²⁶ the broad signals of the ^1H NMR spectra suggest a dynamic equilibrium between different species. This was confirmed by variable-temperature ^1H and ^{31}P NMR studies in the case of the PF_6 salt.²⁶ Recrystallization by slow diffusion of *n*-hexane into a CH_2Cl_2 solution of the crude product yielded dark orange crystals (65 mg). X-ray crystal structure analysis revealed crystallization of $[\text{Cu}_2(\text{dppFc})(\text{dppFc})_2](\text{BF}_4)_2$. ^1H and ^{31}P NMR spectra recorded upon dissolution of these crystals in CD_2Cl_2 were complex and consistent with the presence of different species in solution. This compound was not further investigated.

X-ray Crystal Structures. A. $[\text{Cu}(\text{phen})(\text{dppb})]\text{BF}_4$. Crystals suitable for X-ray crystal structure analysis were obtained by slow diffusion of Et_2O into a CH_2Cl_2 solution of $[\text{Cu}(\text{phen})(\text{dppb})]\text{BF}_4$. Data were collected at 173 K on a Nonius Kappa-CCD diffractometer (Mo $K\alpha$ radiation, $\lambda = 0.71073$ Å). The structure was solved by direct methods (SHELXS-97) and refined against F^2 using the SHELXL-97 software. Non-hydrogen atoms were refined anisotropically using weighted full-matrix least-squares on F^2 . H atoms were included in calculated positions and treated as riding atoms using SHELXL default parameters. Crystallographic data are reported in Table S1, Supporting Information.

B. $[\text{Cu}_2(\text{Bphen})_2(\mu\text{-dppm})_2](\text{BF}_4)_2 \cdot \text{CH}_2\text{Cl}_2$. Crystals suitable for X-ray crystal structure analysis were obtained by slow diffusion of Et_2O into a CH_2Cl_2 solution of $[\text{Cu}_2(\text{Bphen})_2(\mu\text{-dppm})_2](\text{BF}_4)_2$. Data were collected at 173 K on a Nonius Kappa-CCD diffractometer (Mo $K\alpha$ radiation, $\lambda = 0.71073$ Å). The structure was solved by direct methods (SHELXS-97) and refined against F^2 using the SHELXL-97 software. Non-hydrogen atoms were refined anisotropically using weighted full-matrix least-squares on F^2 . H atoms were included in calculated positions and treated as riding atoms using SHELXL default parameters. A semiempirical absorption correction was applied using the MULScanABS routine in PLATON;²⁷ transmission factors, $T_{\text{min}}/T_{\text{max}} = 0.69776/0.84015$. The SQUEEZE instruction in PLATON²⁷ was applied. Residual electron density was assigned to four molecules of dichloromethane. Crystallographic data are reported in Table S1, Supporting Information.

C. $[\text{Cu}(\text{dmp})(\text{dppe})]\text{BF}_4 \cdot \text{Et}_2\text{O}$. Crystals suitable for X-ray crystal structure analysis were obtained by slow diffusion of Et_2O into a CH_2Cl_2 solution of $[\text{Cu}(\text{dmp})(\text{dppe})]\text{BF}_4$. Data were collected at 180 K on a Stoe IPDS diffractometer (Mo $K\alpha$ radiation, $\lambda = 0.71073$ Å). The structure was solved by direct methods (SIR92) and refined against F using the CRYSTALS software. Non-hydrogen atoms were refined anisotropically (excepting the BF_4^- anion and cocrystallized solvent molecule). H atoms were refined as riding atoms constraints. Crystallographic data are reported in Table S1, Supporting Information.

D. $[\text{Cu}(\text{dmp})(\text{dppp})]\text{BF}_4$. Crystals suitable for X-ray crystal structure analysis were obtained by slow diffusion of Et_2O into a CH_2Cl_2 solution of $[\text{Cu}(\text{dmp})(\text{dppp})]\text{BF}_4$. Data were collected at 180 K on a Stoe IPDS diffractometer (Mo $K\alpha$ radiation, $\lambda = 0.71073$ Å). The structure was solved by direct methods (SIR92) and refined against F

using the CRYSTALS software. Non-hydrogen atoms (excepting the BF_4^- anion) were refined anisotropically. Constraints were applied on the phenyl groups. H atoms were refined as riding atoms constraints. Crystallographic data are reported in Table S1, Supporting Information.

E. $[\text{Cu}(\text{POP})_2]\text{BF}_4$. Crystals suitable for X-ray crystal structure analysis were obtained by slow diffusion of *n*-hexane into a CH_2Cl_2 solution of $[\text{Cu}(\text{POP})_2]\text{BF}_4$. Data were collected at 180 K on a Bruker APEX-II CCD diffractometer (Mo $K\alpha$ radiation, $\lambda = 0.71073 \text{ \AA}$). The structure was solved by direct methods (SIR92) and refined against *F* using the CRYSTALS software. Non-hydrogen atoms were refined anisotropically. Thermal constraints were applied on the phenyl groups and BF_4^- anion. H atoms were refined as riding atoms constraints. Crystallographic data are reported in Table S1, Supporting Information.

F. $[\text{Cu}_2(\mu\text{-dppFc})(\text{dppFc})_2](\text{BF}_4)_2 \cdot (\text{CH}_2\text{Cl}_2)(\text{H}_2\text{O})_2$. Crystals suitable for X-ray crystal structure analysis were obtained by slow diffusion of *n*-hexane into a CH_2Cl_2 solution of dppFc (2 equiv) and $\text{Cu}(\text{CH}_3\text{CN})_4\text{BF}_4$ (1 equiv). Data were collected at 180 K on an Oxford Diffraction XCALIBUR diffractometer (Mo $K\alpha$ radiation, $\lambda = 0.71073 \text{ \AA}$). The structure was solved by direct methods (SIR92) and refined against *F* using the CRYSTALS software. Non-hydrogen atoms were refined anisotropically. H atoms were refined with riding constraints. Crystallographic data are reported in Table S1, Supporting Information.

■ ASSOCIATED CONTENT

● Supporting Information

Crystallographic and structure refinement data; crystallographic (CIF) files for $[\text{Cu}(\text{phen})(\text{dppb})]\text{BF}_4$, $[\text{Cu}_2(\text{Bphen})_2(\mu\text{-dppm})_2](\text{BF}_4)_2$, $[\text{Cu}(\text{dmp})(\text{dppe})]\text{BF}_4 \cdot \text{Et}_2\text{O}$, $[\text{Cu}(\text{dmp})(\text{dppp})]\text{BF}_4$, $[\text{Cu}(\text{POP})_2]\text{BF}_4$, and $[\text{Cu}_2(\mu\text{-dppFc})(\text{dppFc})_2](\text{BF}_4)_2 \cdot (\text{CH}_2\text{Cl}_2)(\text{H}_2\text{O})_2$. This material is available free of charge via the Internet at <http://pubs.acs.org>. Final atomic positional coordinates, with estimated standard deviations, bond lengths, and angles, have been deposited at the Cambridge Crystallographic Data Centre and were allocated deposition numbers CCDC 953017, CCDC 953018, CCDC 952426, CCDC 952427, CCDC 952429, and CCDC 972428.

■ AUTHOR INFORMATION

Corresponding Authors

*E-mail: beatrice.delavaux-nicot@lcc-toulouse.fr.

*E-mail: nicola.armaroli@isof.cnr.it.

*E-mail: nierengarten@unistra.fr.

Notes

The authors declare no competing financial interest.

■ ACKNOWLEDGMENTS

This research was supported by the CNRS, the University of Strasbourg, the EC (contract PITN-GA-2008-215399-FINE-LUMEN), MIUR (PRIN 2010 INFOCHEM-CX2TLM), and the CNR (MACOL PM.P04.010 and Progetto Bandiera N-CHEM).

■ REFERENCES

(1) (a) Buckner, M. T.; Matthews, T. G.; Lytle, F. E.; McMillin, D. R. *J. Am. Chem. Soc.* **1979**, *101*, 5846–5848. (b) Rader, R. A.; McMillin, D. R.; Buckner, M. T.; Matthews, T. G.; Casadonte, D. J.; Lengel, R. K.; Whittaker, S. B.; Darmon, L. M.; Lytle, F. E. *J. Am. Chem. Soc.* **1981**, *103*, 5906–5912. (c) Del Paggio, A. A.; McMillin, D. R. *Inorg. Chem.* **1983**, *22*, 691–692. (d) Kirchhoff, J. R.; McMillin, D. R.; Robinson, W. R.; Powell, D. R.; McKenzie, A. T.; Chen, S. *Inorg. Chem.* **1985**, *24*, 3928–3933. (e) Casadonte, D. J.; McMillin, D. R. *Inorg. Chem.* **1987**, *26*, 3950–3952. (f) Palmer, C. E. A.; McMillin, D. R. *Inorg. Chem.* **1987**, *26*, 3837–3840.

(2) (a) Sakaki, S.; Koga, G.; Ohkubo, K. *Inorg. Chem.* **1986**, *25*, 2330–2333. (b) Sakaki, S.; Koga, G.; Hinokuma, S.; Hashimoto, S.; Ohkubo, K. *Inorg. Chem.* **1987**, *26*, 1817–1819.

(3) Cuttall, D. G.; Kuang, S.-M.; Fanwick, P. E.; McMillin, D. R.; Walton, R. A. *J. Am. Chem. Soc.* **2002**, *124*, 6–7.

(4) Kuang, S.-M.; Cuttall, D. G.; McMillin, D. R.; Fanwick, P. E.; Walton, R. A. *Inorg. Chem.* **2002**, *41*, 3313–3322.

(5) (a) Coppens, P. *Chem. Commun.* **2003**, 1317–1320. (b) Coppens, P.; Vorontsov, I. I.; Graber, T.; Kovalevsky, A. Y.; Chen, Y.-S.; Wu, G.; Gembicky, M.; Novozhilova, I. V. *J. Am. Chem. Soc.* **2004**, *126*, 5980–5981. (c) Saito, K.; Arai, T.; Takahashi, N.; Tsukuda, T.; Tsubomura, T. *Dalton Trans.* **2006**, 4444–4448.

(6) Costa, R. D.; Tordera, D.; Orti, E.; Bolink, H.; Schönle, J.; Graber, S.; Housecroft, C. E.; Constable, E. C.; Zampese, J. A. *J. Mater. Chem.* **2011**, *21*, 16108–16118.

(7) (a) Linfoot, C. L.; Richardson, P.; Hewat, T. E.; Moudam, O.; Forde, M. M.; Collins, A.; White, F.; Robertson, N. *Dalton Trans.* **2010**, 39, 8945–8956. (b) Zhang, Q.; Zhou, Q.; Cheng, Y.; Wang, L.; Ma, D.; Jing, X.; Wang, F. *Adv. Mater.* **2004**, *16*, 432–436. (c) Zhang, Q.; Zhou, Q.; Cheng, Y.; Wang, L.; Ma, D.; Jing, X.; Wang, F. *Adv. Funct. Mater.* **2006**, *16*, 1203–1208. (d) MacCormick, T.; Jia, W.-L.; Wang, S. *Inorg. Chem.* **2006**, *45*, 147–155. (e) Ge, H.; Wei, W.; Shuai, P.; Lei, G.; Qing, S. *J. Lumin.* **2011**, *131*, 238–243.

(8) Armaroli, N.; Accorsi, G.; Holler, M.; Moudam, O.; Nierengarten, J.-F.; Zhou, Z.; Wegh, R. T.; Welter, R. *Adv. Mater.* **2006**, *18*, 1313–1316.

(9) Yang, L.; Feng, J.-K.; Ren, A.-M.; Zhang, M.; Ma, Y.-G.; Liu, X.-D. *Eur. J. Inorg. Chem.* **2005**, 1867–1879.

(10) Armaroli, N.; Accorsi, G.; Bergamini, G.; Ceroni, P.; Holler, M.; Moudam, O.; Duhayon, C.; Delavaux-Nicot, B.; Nierengarten, J.-F. *Inorg. Chim. Acta* **2007**, *360*, 1032–1042.

(11) Moudam, O.; Kaeser, A.; Delavaux-Nicot, B.; Duhayon, C.; Holler, M.; Accorsi, G.; Armaroli, N.; Séguy, I.; Navarro, J.; Destruel, P.; Nierengarten, J.-F. *Chem. Commun.* **2007**, 3077–3079.

(12) Listorti, A.; Accorsi, G.; Rio, Y.; Armaroli, N.; Moudam, O.; Gégout, A.; Delavaux-Nicot, B.; Holler, M.; Nierengarten, J.-F. *Inorg. Chem.* **2008**, *47*, 6254–6261.

(13) Mohankumar, M.; Holler, M.; Nierengarten, J.-F.; Sauvage, J.-P. *Chem.—Eur. J.* **2012**, *18*, 12192–12195.

(14) Dietrich-Buchecker, C. O.; Marnot, P. A.; Sauvage, J.-P. *Tetrahedron Lett.* **1982**, *23*, 5291–5294.

(15) Gumienna-Kontecka, E.; Rio, Y.; Bourgogne, C.; Elhabiri, M.; Louis, R.; Albrecht-Gary, A.-M.; Nierengarten, J.-F. *Inorg. Chem.* **2004**, *43*, 3200–3209.

(16) Gschwind, R. M. *Chem. Rev.* **2008**, *108*, 3029–3053.

(17) (a) Puddephatt, R. J. *Chem. Soc. Rev.* **1983**, *12*, 99–127. (b) Chaudret, B.; Delavaux, B.; Poilblanc, R. *Coord. Chem. Rev.* **1988**, *86*, 191–243.

(18) (a) Harvey, P. D.; Drouin, M.; Zhang, T. *Inorg. Chem.* **1997**, *36*, 4998–5005. (b) Bera, J. K.; Nethaji, M.; Samuelson, A. C. *Inorg. Chem.* **1999**, *38*, 218–228. (c) Deivaraj, T. C.; Vittal, J. J. *J. Chem. Soc., Dalton Trans.* **2001**, 322–328. (d) Yang, R.-N.; Sun, Y.-A.; Hou, Y.-M.; Hu, X.-Y.; Jin, D.-M. *Inorg. Chim. Acta* **2000**, *304*, 1–6. (e) Ruina, Y.; Kunhua, L.; Yimin, H.; Dongmei, W.; Douman, J. *Polyhedron* **1997**, *16*, 4033–4038. (f) Yang, R.; Liu, Y.; Jin, D. *J. Coord. Chem.* **2002**, *55*, 179–188.

(19) Wei, Y.-Q.; Wu, K.-C.; Zhuang, B.-T.; Zhou, Z.-F. *J. Coord. Chem.* **2006**, *59*, 713–719.

(20) (a) James, B. R.; Williams, R. J. P. *J. Chem. Soc.* **1961**, 2007–2019. (b) Arnaud-Neu, F. A.; Marques, E.; Schwing-Weill, M.-J.; Dietrich-Buchecker, C. O.; Sauvage, J.-P.; Weiss, J. *New J. Chem.* **1988**, *12*, 15–20.

(21) McMillin, D. R.; Buckner, M. T.; Ahn, B. T. *Inorg. Chem.* **1977**, *16*, 943–945.

(22) Comba, P.; Katsichtis, C.; Nuber, B.; Pritzkow, H. *Eur. J. Inorg. Chem.* **1999**, 777–783.

(23) (a) Riesgo, E.; Hu, Y.-Z.; Bouvier, F.; Thummel, R. P. *Inorg. Chem.* **2001**, *40*, 2541–2546. (b) Pianet, I.; Vincent, J.-M. *Inorg. Chem.* **2004**, *43*, 2947–2953. (c) Hebbe-Viton, V.; Desvergnès, V.; Jodry, J.

J.; Dietrich-Buchecker, C.; Sauvage, J.-P.; Lacour, J. *Dalton Trans.* **2006**, 2058–2065.

(24) De, S.; Mahata, K.; Schmittel, M. *Chem. Soc. Rev.* **2010**, 39, 1555–1575.

(25) Venkateswaran, R.; Blakrishna, M. S.; Mobin, S. M.; Tuononen, H. M. *Inorg. Chem.* **2007**, 46, 6535–6541.

(26) Long, N.; Martin, J.; Opromolla, G.; White, A. J. P.; Williams, D. J.; Zanello, P. J. *Chem. Soc., Dalton Trans.* **1999**, 1981–1986.

(27) Spek, A. L. *J. Appl. Crystallogr.* **2003**, 36, 7–13.